Aalborg Universitet

AALBORG UNIVERSITY

DENMARK

Comparative study of the break in process of post doped and sol–gel high temperature proton exchange membrane fuel cells

Vang, Jakob Rabjerg; Andreasen, Søren Juhl; Simon Araya, Samuel; Kær, Søren Knudsen

Comparative study of the break in process of post doped and sol-gel high temperature proton exchange membrane fuel cells

Jakob Rabjerg Vang[a,*], Søren Juhl Andreasen[a], Samuel Simon Araya[a], Søren Knudsen Kær[a]

[a]*Department of Energy Technology, Aalborg University, Pontoppidanstræde 101, 9220 Aalborg East, Denmark*

Abstract

In this paper six High Temperature PEM (HTPEM) MEAs from two manufacturers have been tested. The MEAs are three Dapozol 77 from Danish Power Systems (DPS) with varying electrode composition and two Celtec P2100 and one Celtec P1000 from BASF. The break in process of the MEAs has been monitored using voltage measurements and impedance spectroscopy. The purpose of this study is twofold. One aim is to try and interpret the processes happening during break in. The other aim is to investigate whether the impedance spectra or the voltage profiles contain information that can be used to determine when a MEA has been broken in. To aid in the interpretation of the impedance spectra, equivalent circuit models are used. Three models are evaluated. The most detailed models produce the best fits but the most simple model is chosen, since it produces the most consistent results. The processes happening during break in cannot be determined with certainty but for the Celtec P MEAs the main changes seem to be related to improved electrode kinetics. Judging from the voltage and the fitted resistances, the Celtec P MEAs seem to have been broken in after 30 hours. The Dapozol MEAs only undergo minor changes in impedance and voltage during the break in period. This may indicate that this MEA type can be used directly without the need for break in.

Keywords: High temperature PEM fuel cell; Impedance spectroscopy; Break in; Dapozol; Celtec; Equivalent circuit model

1. Introduction

The use of high temperature proton exchange membrane (HTPEM) fuel cells based on phosphoric acid (PA) doped polybenzimidazole (PBI) is advantageous for a number of reasons, including high impurity tolerance, no water management issues and easy cooling and high quality waste heat due to the high operating temperature. The challenges to be overcome on the road to widespread commercialisation of this technology are, however, still substantial.

The focus of this work is the initial activation or break in, which must be performed before subjecting the cell to high loads, in order to achieve maximum performance and durability. The break in is generally carried out by running the cell at a low galvanostatic load for around 100 hours [1–4]. Lobato et al. [5] used potentiostatic conditioning at 0.5 V for 25 hours. Other approaches have been tried, including potential cycling [2, 4] and start/stop operation [1] but these have not been found to be suitable. Tingelöf and Ihonen [4] suggested that galvanostatic break in could be performed at 200 °C for a short time with a subsequent longer relaxation period at the required operating temperature. This method resulted in reproducible performance

but the performance was slightly worse than when doing galvanostatic break in at 160 °C. Lobato et al. [5] tested the effect of different break in temperatures and found that high temperature break in reduced performance through dehydration of the membrane.

In this work, performance during galvanostatic break in of two different types of MEAs is monitored using electrochemical impedance spectroscopy (EIS). EIS is chosen, since the impedance spectrum can be recorded without changing the operating point as would be necessary if polarisation curves were used. The aim of this work is to interpret the processes happening during break in of the MEAs and investigate the possibility for shortening galvanostatic break in times without compromising fuel cell performance.

This work investigates the break in process of two different types of HTPEM MEAs. One type is the Dapozol 77 from Danish Power systems (DPS) in which the PBI membrane is doped by submersion in H_3PO_4 after casting from a DMAc solution. This method is similar to the one used by Wainright et al. [6] for producing the first PBI based HTPEM fuel cell. According to the manufacturer, the doping level was 9 H_3PO_4 molecules per PBI repeat unit. The catalyst layer was prepared with a Pt/carbon catalyst with 60 wt.% Pt, using PBI as binder. The loading of Pt and the C/PBI ratio was varied as specified in table 1. The C/PBI ratio was masked by normalising by the lowest value used. The table also gives the naming convention used

---

*Corresponding Author. Tel: +4521369289

Email addresses: `jrv@et.aau.dk` (Jakob Rabjerg Vang), `sja@et.aau.dk` (Søren Juhl Andreasen), `ssa@et.aau.dk` (Samuel Simon Araya), `skk@et.aau.dk` (Søren Knudsen Kær)

for the MEAs. The other MEAs were two Celtec P2100 and one Celtec P1000 from BASF. These MEAs were manufactured using a sol-gel process as described by Xiao et al. [7]. This process results in membranes with doping levels up to 70 H_3PO_4/PBI [8]. Information regarding the Pt/C ratio of the catalyst and the binder type and loading of the Celtec P MEAs was unavailable.

MEA name	MEA type	Cathode Pt loading	Normalised C/PBI wt. ratio in CL	Cell area
DPS1	Dapozol 77	$0.98\,\mathrm{mg/cm^2}$	1	$46\,\mathrm{cm^2}$
DPS2	Dapozol 77	$0.98\,\mathrm{mg/cm^2}$	1.22	$46\,\mathrm{cm^2}$
DPS3	Dapozol 77	$0.8\,\mathrm{mg/cm^2}$	1	$46\,\mathrm{cm^2}$
BASF1	Celtec P2100	–	–	$45\,\mathrm{cm^2}$
BASF2	Celtec P2100	–	–	$45\,\mathrm{cm^2}$
BASF3	Celtec P1000	$0.75\,\mathrm{mg/cm^2}$[8]	–	$45\,\mathrm{cm^2}$

Table 1: Data for the MEAs used and the names used to refer to them in the text.

2. Experimental

The MEAs were tested in the fuel cell laboratory at the Department of Energy Technology at Aalborg University. A drawing of the experimental set-up is shown in figure 1. The MEAs were installed in a single cell unit with graphite composite flow plates with serpentine flow fields. The current collector plates were made from brass and the end plates from steel. The fuel cell temperature was controlled using resistance heaters installed in the end plates. The temperature was measured by two thermocouples inserted into the flow plates. The reactant flow was controlled using Bürkert mass flow controllers (MFCs). Two LabView real-time PCs were connected to the set-up. The FC control PC controlled the operating conditions and logged both set points and measured values of the variables. The EIS PC was employed to generate the impedances spectrum. A list of the equipment used, and the accuracy and bias error associated with each piece of equipment is given in table 2.

Break in was performed at 160°C. The load current was 9 A for all MEAs, corresponding to approximately $0.2\mathrm{A/cm^2}$ for both MEA types. The cathode was fed ambient air and the anode was fed pure, dry hydrogen. The stoichiometries were 4.4 for the cathode and 1.3 for the anode. All reactants were fed at ambient pressure.

The voltage was logged continuously and impedance spectra were recorded at regular intervals throughout the break in period. Break in was terminated after a minimum of 90 hours, when the rate of change in the voltage and/or the impedance spectra had stabilised. Due to a combination of human error and bugs in the LabView code controlling the set-ups, voltage and/or impedance data is missing from parts of some of the break in datasets. Table 3 shows the time span of the data for each MEA.

Equipment	Model	Range	Accuracy	Bias error
Air MFC	Bürkert 8712	0.04 - 2 $\frac{l_N}{min}$	±0.8%	±0.3%
H_2 MFC	Bürkert 8711	0.02 - 1 $\frac{l_N}{min}$	±0.8%	±0.3%
Load	RBL488 50-150-800	0 - 150 A	±0.25	±0.1%
Thermocouples	AMETEK 1500 MT4 - Type T	-40 - 400°C	±0.4%	±0.125%
FC ctrl PC AI	NI 6229	0 - 10 V	±0.015%	±0.015%
FC ctrl PC AO	NI 6704	0 - 10 V	± > 0.01	±0.007%
EIS PC AI	NI 6229	0 - 10 V	±0.015%	±0.015%
EIS PC AO	NI 6229	0 - 10 V	±0.015%	±0.017%

Table 2: Overview of the equipment used and the associated uncertainty. Accuracy refers to the measured/specified value. Bias errors refer to full scale values.

MEA	Data Voltage	Impedance	Comment
DPS1	0-138 h	0-137 h	
DPS2	0-118 h	66-118 h	A bug in the LabView EIS software corrupted all spectra before 66 hours.
DPS3	-	0-108 h	Due to a human error, the voltage data was not recorded
BASF1	0-116 h	4-113 h	The spacing between the EIS points is larger than for the other MEAs
BASF2	0-98 h	0-96 h	
BASF3	0-94 h	0-94 h	

Table 3: Overview of the available break in data for each of the MEAs.

3. Results and discussion

In this section, the data extracted during the break in period is presented and discussed. The data was recorded at different points in time when a new MEA was installed and broken in prior to characterisation. Some details in the handling of the MEAs may have changed between tests. As seen in the following, some variation indicates that this may have affected the results. There are, however, trends in the development of the impedance of the fuel cells, which are common to all MEAs. These suggest that some of the processes happening are independent of manufacturing process.

3.1. Voltage profiles

The most straight forward way of monitoring the fuel cell during galvanostatic break in is to monitor the development of the voltage. Figure 2 shows the voltage development of the individual MEAs during the break in period as well as the voltage and temperature during the first 20 hours. As can be seen from figures 2a and 2b, the cell voltage changes during break in. To remove the variations introduced by the impedance measurements, a linear filter with a window of 1 h has been applied. The performance of the individual cells as well as the trends shown by the
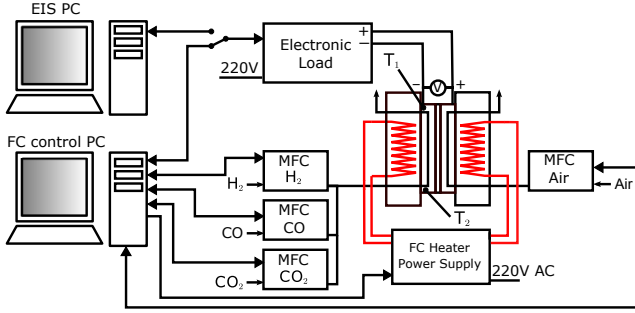
Figure 1: Schematic of the experimental set-up.

voltages are substantially different. One significant detail is the difference between the voltage trend of the MEAs made by BASF and those made by DPS. The Celtec P MEAs all exhibit a significant performance increase of up to 20 mV during the first 20 hours of break in, after which the performance either starts decreasing (BASF1), levels out (BASF2) or keeps increasing at a slower rate (BASF3). The Dapozol MEAs both show a small drop in voltage during the first hour of break in after which the performance gradually levels out. The DPS2 voltage drops the most steeply until around 30 hours and then starts increasing again. The DPS1 voltage decreases steadily for a longer time and only starts increasing around 80 hours. After the first hour, the voltage of each MEA stays within a window of 0.01V. One detail, that is common to most of the MEAs, independent of manufacturer, is an initial decrease of the voltage during the first hour. As can be seen in figure 2b, this decrease can be detected in all the MEAs, but it is not as pronounced in the BASF1 and BASF2 MEAs.

The differences in behaviour can to some extend be explained by the MEAs being different by design. This must be the case for the difference in the initial behaviour between the Celtec P MEAs and the Dapozol MEAs. The lack of consistency between the development exhibited by MEAs of the same manufacture and even supposedly identical MEAs from the same batch (BASF1 and BASF2) is probably a result of one or more of the following factors:

3.1.1. Problems with quality in MEA production

Published microscopy pictures of HTPEM MEAs [9–11] show local variations in membrane and catalyst layer thickness and even de-lamination of catalyst layers. This indicates that accurately controlling the production of the catalyst layers may be challenging. This may impact the performance of the MEAs.

3.1.2. Variations between experiments

Since the MEAs were placed in the test stand by hand, misalignment of the MEA relative to the gaskets and the flow field may occur. Also, the MEAs were subjected to different ambient conditions when they were installed. The different MEAs were tested consecutively during a period from April to January. As the laboratory tends to get
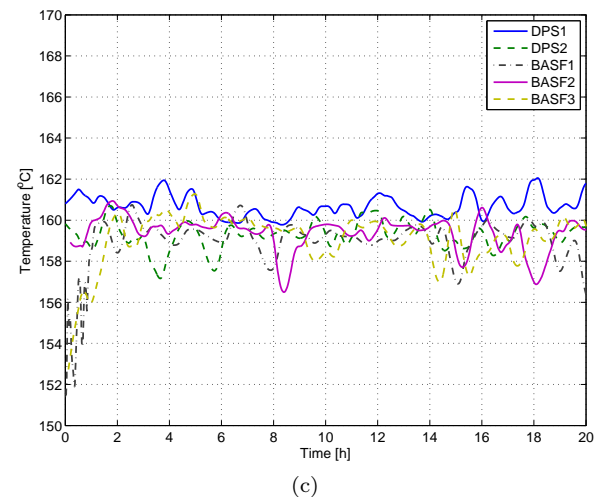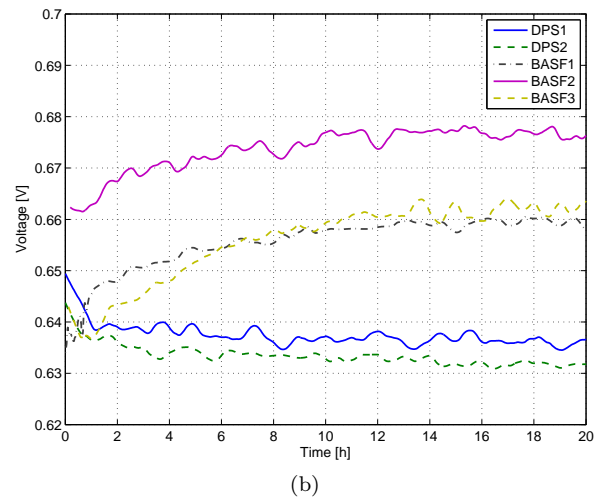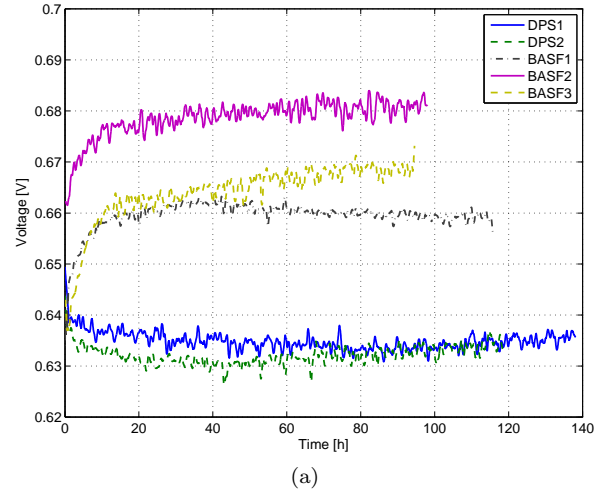

(a)

(b)

(c)

Figure 2: Development of the cell voltages during the break in period (a), detailed view of the voltage development during the first 20 hours (b), and the development of the cell temperatures during same 20 hours (c).

rather hot during summer, the difference in ambient tem-

perature may have been up to 20 °C. This may have affected the performance of the individual cells. Galbiati et al. [1] demonstrated a performance loss similar to the voltage difference between the BASF1 and BASF2 MEAs by subjecting a Celtec P2100 MEA to ambient conditions for 1 hour prior to break in. Differences in time between installation and start of break in could well be the reason for the observed performance variations between BASF1 and BASF2.

The effect of the ambient conditions during operation should also be considered. The difference between the inlet temperature and the operating temperature changes by 15% when going from 15°C to 35°C. This would only effect a small part of the cell near the inlet, since the air is quickly heated inside the narrow flow channels. Humidity is another factor. If 50% humidity is assumed, the difference in outlet water mole fraction is ~15% between 15°C and 35°C. The effects of these variations are assumed to be within acceptable limits.

3.1.3. Problems with control of experimental variables

The main difficulty in this respect is the control of the operating temperature of the fuel cell. The design of the system makes accurate temperature control difficult. The temperature is kept reasonably close to the set point value of 160 °C. Short term variations as large as 10 °C do occur, however. Figure 2c shows the temperature development during the first 20 hours filtered in the same way as the voltage data. Comparing figures 2b and 2c, the oscillations of the temperature and the voltage are correlated for each MEA.

3.2. Post break in performance

After completing the break in, the individual cells have been characterised by running polarisation and impedance spectra at different temperatures and anode gas compositions. Generally, the measurement sequence was started directly after completing the break in sequence without shutting down the fuel cell. The exception from this rule was the DPS1 MEA. Due to problems with the script used for recording the polarisation curve, no polarisation data was collected when the script was run just after break in. The fuel cell was shut down while the system was debugged. This means that the first polarisation curves were only recorded two weeks after finishing the break in. Also, the cell was subjected to carbon monoxide in the anode feed during the measurement sequence.

Figure 3 shows polarisation curves for each MEA at 160 °C. For the BASF2 and BASF3 MEAs two polarisation curves have been recorded subsequently at the same operating conditions to give an idea of the experimental variation. The voltage differences shown in figure 2a are reproduced in the polarisation curves. The performance of the BASF1 MEA has evidently been compromised given the much steeper slope compared to the BASF2 and BASF3 MEAs. The performance of the Dapozol MEAs is

around 50 mV lower than the best Celtec P MEA. Due to the problems with the characterisation of the DPS1 MEA, the effects of the differences in electrode parameters cannot be readily established. The best performance amongst the DPS MEAs is exhibited by the DPS2 MEA. This is to be expected, since higher C/PBI ratio and higher catalyst loading both has been shown to improve performance. Given that the catalyst loading of the DPS1 MEA is higher compared to that of the DPS3 MEA, the performance of the former should be expected to be better. As can be seen from the figure, this is not the case for the polarisation curve recorded 2 weeks after break in. Interestingly, the one recorded after 6 weeks shows better performance.
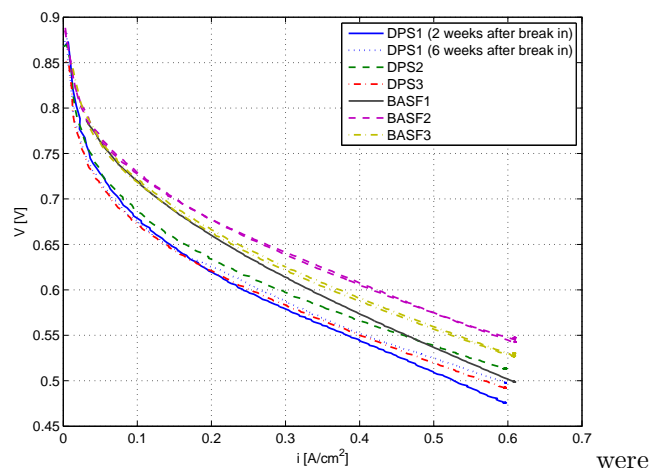

Figure 3: Polarisation curves recorded after break in at 160 °C.

3.3. Impedance spectra

In order to determine the processes occurring during break in, it is worthwhile to have an idea about what the different parts of the impedance spectrum represent. In this way it is possible to analyse the changes occurring during the break in process.

The impedance spectrum is the result of a number of interacting inductive, capacitive and resistive contributions. The contributions can be visualised by looking at the Nyquist plot of a spectrum. The number of contributions depend on the spectrum in question. Figure 4 shows examples of impedance spectra from a Celtec P2100 and a Dapozol 77 MEA. The spectra of both MEA types can be approximated as a combination of three capacitive loops, two inductive loops and one pure ohmic contribution.

The ohmic contribution is responsible for moving the high frequency intercept of the spectrum with the real axis towards the right. The ohmic contribution is related to resistances in the fuel cell. The most prominent is the resistance to proton transport in the membrane, but contact resistances between the individual cell components can also be significant.

The inductive and capacitive contributions are denoted by the relative frequency at which they appear in the

were

4

spectrum. The capacitive contributions are denoted as high, intermediate and low frequency respectively. The high frequency contribution is visible around the 100 Hz mark in the left of both spectra. This contribution is more pronounced in the Celtec P2100 MEA. This loop is attributed either to the effects of limited catalyst layer conductivity [12] or to anode activation [13]. The intermediate frequency contribution is the most prominent loop in the Nyquist plot, primarily associated with cathode activation. The top point of the resulting loop is located slightly left of the 10 Hz mark in the spectrum of the Celtec P MEA and to the right of the 10 Hz mark in the Dapozol MEA spectrum. The low frequency capacitive loop becomes visible just left of the 1 Hz mark. In the spectrum of the Dapozol MEA, the low frequency capacitive loop and the intermediate frequency loop partially overlap. This contribution is related to some kind of mass transport limitation. The exact nature of this limitation is debated. Some sources attribute it to diffusion in the gas diffusion layer and the catalyst layer [14], while others claim it to be a result of gas channel dynamics [15–17].

The inductive contributions are visible in either end of the Nyquist plot, where the spectrum crosses below the real axis. The high frequency inductive contribution is located in the left-most part of the spectrum. This contribution pulls the intersection of the spectrum with the real axis slightly to the right. This contribution can be attributed to the inductance of wires and other components in the fuel cell [11]. In the case of the present measurements, the contribution is probably related to the current collector plates in the set-up, since running the same set-up with a new set of plates has almost eliminated this inductive loop. The low frequency inductive loop is visible around the 0.1 Hz mark. This contribution can be attributed to the formation of intermediates in the electrode reactions [18, 19].

It is important to keep in mind that this division of the impedance spectrum into six distinct contributions is a simplification. Each of the contributions are in itself a combination of many smaller contributions and some effects overlap. The spectrum also averages the large spatial variations in impedance within the fuel cell. These are mainly related to differences in reactant partial pressure [15, 16].

3.3.1. Equivalent circuit model selection

The impedance data has been fitted to equivalent circuit models in order to get a more quantitative measure of the changes during break in of the fuel cells and to get an idea about the processes happening during break in. The models are made up of ideal electrical components in an attempt to capture the contributions outlined in the section 3.3.

Since equivalent circuit models only mimic the electrical behaviour of the fuel cell without considering the processes happening within, it is worthwhile testing if similar results can be obtained with different models. The
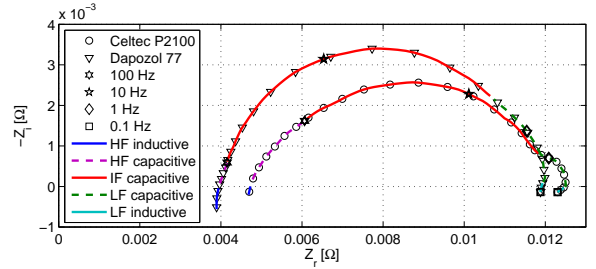

Figure 4: Break down of the impedance spectrum of a Celtec P2100 and a Dapozol 77 MEA into individual contributions. Abbreviations: HF - high frequency, IF - intermediate frequency, LF - low frequency.

three models compared are shown in figure 5. The models are mostly similar. The ohmic contribution is represented by the ohmic resistance R_Ω. An inductor with inductance L_{HF} represents the high frequency inductive contribution. The high frequency capacitive loop is modelled by a parallel combination of the resistance R_{HF} and a constant phase element (CPE) with pseudo-capacitance Q_{HF}. The CPE exponent ϕ is set to 0.5 to give the initial 45° slope often observed in Nyquist plots of fuel cell impedance spectra [12]. A capacitor with capacitance C_{IF} and the resistor R_{IF} form the intermediate frequency loop. The low frequency inductive loop is represented by a parallel RL circuit with resistance $R_{I,LF}$ and inductance L_{LF}. R_Ω and $R_{I,LF}$ both count towards the displacement of the high frequency intercept. Between individual fits, the degree to which each of them contribute may vary greatly due to the noisy nature of the low frequency part of the impedance spectra. The sum $R_{RES} = R_\Omega + R_{I,LF}$ is very consistent, however, and thus this value is used when plotting the development of the ohmic contribution.

Models 1 and 2 differ in the way the low frequency capacitive loop is modelled. Model 1 represents this loop by a parallel RC circuit similar to that used for the intermediate frequency loop. Model 2 uses a bounded Warburg element with Warburg coefficient R_W inserted in series with R_{IF} to form a modified Randles circuit. Model 3 is similar to Model 2 except that the high frequency part is ignored and that the intermediate frequency loop is modelled using a CPE with $\phi = 0.8$. The formulations used for CPEs and Warburg impedances are given in (1) and (2).

$$Z_{CPE} = \frac{1}{Q(j2\pi f)^\phi} \tag{1}$$

$$Z_W = R_w \frac{\tanh\left(T_w\,(j2\pi f)^{\,0.5}\right)}{T_w\,(j2\pi f)^{\,0.5}} \tag{2}$$

To compare the models, they have each been fitted to the impedance data from the BASF 2 MEA. Figure 6 shows an example of how the models fit the impedance spectrum. Models 1 and 2 fit the data well, with an average RMS deviation between models 1 and 2 and the data of
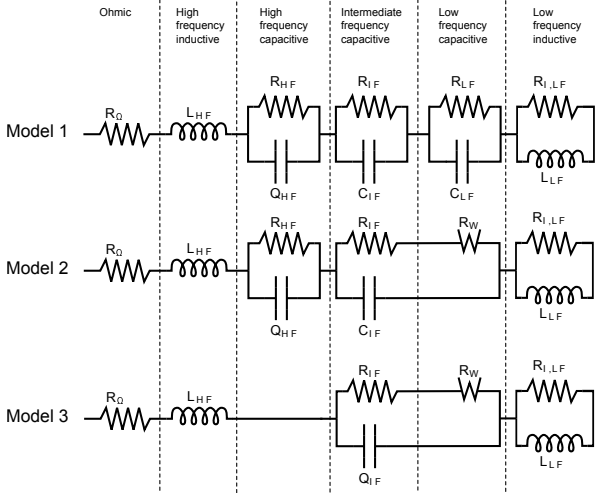
Figure 5: The equivalent circuit models used for fitting the impedance data.

1.86%. Model 3 does not fit the data quite as well, since it does not take into account the high frequency capacitive loop. The average RMS deviation between model 3 and the data is 2.14%.
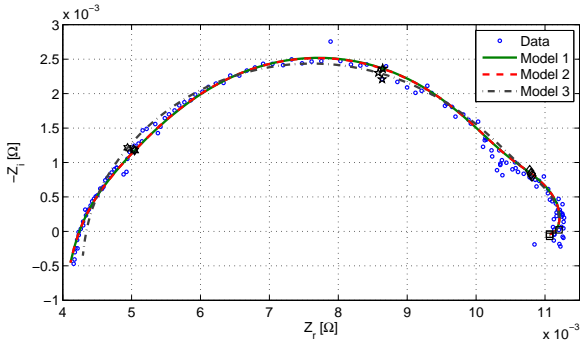

Figure 6: Comparison of the fit quality for Models 1, 2 and 3 applied to the BASF2 impedance spectrum 27 hours into the break in process.

Figures 7 and 8 show the development of the fitted resistances for each of the models to the BASF2 data. Figure 7 shows the development throughout the break in period, while figure 8 shows the first 20 hours. Trend lines are plotted by fitting the resistances to an expression of the form

$$R = a + b \exp(ct) + dt \qquad (3)$$

where R [Ω] is the resistance, t [h] is time, and a, b, c, and d are fitting coefficients.

The resistance values extracted differ among the models. The ohmic contribution seems to be the least affected by the choice of model. Models 1 and 2 produce very similar values. Model 3 produces R_{RES} values that are on average 17.5% higher. The trend is, however, identical for all models. R_{RES} increases throughout the break in period at a gradually decreasing rate.

The values of R_{HF} are more model dependent. The trend lines indicate, that R_{HF} starts by falling and then levels out. $R_{HF,2}$ seems to be falling for a longer time before levelling out. Otherwise the development trend is similar for the two models. It should be noted that the scatter of the data points makes it difficult to determine if the difference is significant.

R_{IF} is smaller than R_{HF} for both models 1 and 2. This seems counter intuitive, since the high frequency loop visible in the Nyquist plot is much smaller than the intermediate frequency loop. The development of $R_{IF,1}$ and $R_{IF,2}$ show an initial decrease and subsequent levelling out. The difference between $R_{IF,1}$ and $R_{IF,2}$ is less than between $R_{HF,1}$ and $R_{HF,2}$ and the scatter of the data points is less. Since there is no $R_{HF,3}$, $R_{IF,3}$ spans both the low and intermediate frequency loops. To better enable comparison, $R_{HF} + R_{IF}$ are plotted for models 1 and 2. The most notable feature of $R_{IF,3}$ is the consistency of the data points. The trend of the development is clear, with a strong initial decrease and subsequent levelling out with hardly any change after 30 hours.

The values of R_{LF} and R_W are quite scattered for all three models. Models 1 and 2 have more scatter than model 3. The values all exhibit a slight increase over the course of the break in process.

Considering the lack of consistency in the fitted values produced by models 1 and 2, model 3 seems the best option for monitoring the changes in the impedance during break in. However, the significant degree to which the fitted resistances depend on the model, the scatter in the fitted values, and the fact that it is possible to obtain different values by varying the initial guess, indicate that the simple equivalent circuit models used in this study can only give a general idea of the processes happening during break in. The model might, however, help to determine when break in can be terminated by observing the changes in the individual fitted resistances.
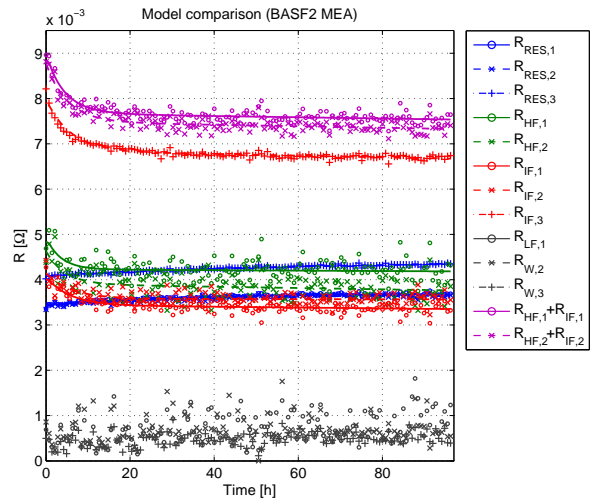

Figure 7: Fitted resistance values with trend lines for models 1, 2 and 3 applied to the BASF2 MEA data set.
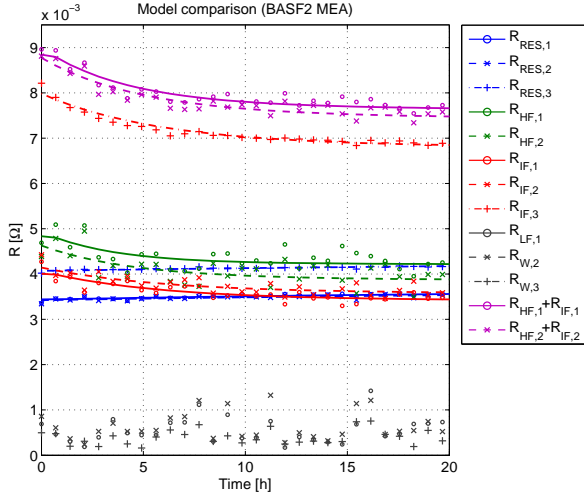
Figure 8: Fitted resistance values with trend lines for models 1, 2 and 3 applied to the BASF2 MEA data set for the first 20 hours of break in.

3.3.2. MEA comparison

In this section the development of the resistances extracted by fitting model 3 to the data of each MEA are compared and discussed. The processes happening during break in are discussed and an attempt is made to identify criteria for when a MEA can be considered broken in. As with the voltage development, the Celtec P and Dapozol MEAs have different characteristics which most likely relate to the differences in the manufacturing processes.

Ohmic resistance. A plot of the fitted ohmic resistances as a function of time can be seen if figure 9. The general trend for the ohmic resistance is increasing. This is in agreement with the observation that the high frequency intercept of the curve with the real axis in the Nyquist plot moves to the right during the break in period. The effect is most pronounced at the beginning of the break in period and gradually levels off. The ohmic resistance of the BASF3 MEA seems to shrink within the first 10 hours and then increase in the same way as the other MEAs. The BASF1 and BASF3 MEAs seem to reach a maximum value of R_{RES} at around 50 hours, after which the value remains approximately constant. This could perhaps indicate that the break in process is complete for these MEAs after 50 hours. Since the BASF1 and BASF2 MEAs behave differently in this respect, the conclusion is uncertain, however. The development of R_{RES} differ from the observations of Galbiati et al. [1] who observed a logarithmic decrease of the membrane resistance during break in, which was correlated to the increase in cell voltage.

The increasing ohmic resistance can most likely be explained by gradual dehydration of the PA in the membrane. The most important variables for PA conductivity are temperature and water content. At a water content below 50% by weight, conductivity increases with water

content [20]. While high temperatures increase the conductivity of PA, the vapour pressure of the water in the PA also increases [21]. This means that unless the cell is hydrated, the ohmic resistance will continue to increase as the cell dries. The discrepancy between the development of the ohmic resistance observed by Galbiati et al. [1] and the development in this work can thus be explained by the difference in air stoichiometry. Galbiati and co-workers used a value of 2, while a value of 4.4 was used in this work. This means that the average water content in the cathode channel in this case should generally be lower than in the work of Galbiati et al. This can be supposed to lead to faster and more severe dehydration. This phenomenon could be countered either by humidifying the reactant gasses [22] or by shutting down the cell, letting it cool and waiting until the water balance is re-established at ambient conditions.

Another reason for part of the increase in ohmic resistance could be acid redistribution. The PA in a HTPEM fuel cell is quite mobile and can move back and forth between the membrane and the catalyst layers [3, 23]. The mobility of the PA could theoretically lead to acid loss through the GDL and a permanent increase in the ohmic resistance. This contribution is probably not significant, however, since Yu et al. [24] demonstrated PA loss rates on the order of ng/$(cm^2 h)$ corresponding to a few % loss during a hypothetical life time of 40.000 hours.
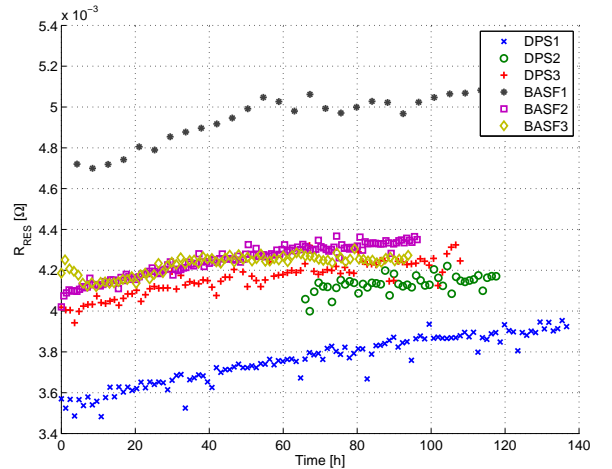

Figure 9: Fitted values of $R_\Omega + R_{I,LF}$ vs. time. Results from fitting model 3.

Intermediate frequency resistance. The modelling of the intermediate frequency capacitive loop is slightly different for the Dapozol and the Celtec P MEAs. Due to the differences in shape of the impedance spectra the value used for ϕ is 0.8 for the Celtec P MEAs and 0.95 for the Dapozol MEAs.

Figure 10 shows the development of R_{IF} for each of the MEAs tested. The development of the intermediate frequency resistance to some extent reflects the development of the cell voltage during break in. This is at least true for the Celtec P MEAs during the first 20 to 30 hours.

Here the decrease in resistance evident in figure 10 occurs at the same time as the increase in voltage in figure 2a. Since both voltage and R_{IF} levels out after 30 hours the Celtec P MEAs seem to be broken in after 30 hours. Convergence of R_{IF} seems to be more consistent between the Celtec P MEAs than the convergence of the voltage. This indicates that monitoring R_{IF} can be a useful supplement to monitoring the voltage when determining break in of Celtec P MEAs. Similar results for the development of R_{IF} for Celtec P2100 MEAs were obtained by Galbiati et al. [1].

The R_{IF} values for the Dapozol MEAs decrease more or less linearly with time. When comparing with figure 2a, the voltage of the DPS1 and DPS2 MEAs also drops more or less linearly during the time where both voltage and impedance data are available. Thus, there is no distinct feature in R_{IF} for the Dapozol MEAs that could indicate when break in can be terminated. On the other hand, the lack of convergent behaviour might signify that the Dapozol MEAs need none, or only limited break in.

The decreasing trends in the intermediate frequency resistance indicates that the electrodes become more active in all the MEAs during the break in process. This could be a result of improved PA distribution, which in turn leads to a larger triple phase boundary and larger electrode active area. Assuming that redistribution of PA is the main cause for the decrease in R_{IF}, the larger change observed for the Celtec P MEAs can be explained by large amounts of PA blocking some of the CL pores at the start of break in.

In order to test the potential for shortening or eliminating break in of Celtec P as well as Dapozol MEAs, direct comparison of the short term and long term performance of MEAs subjected to different break in times will be needed.
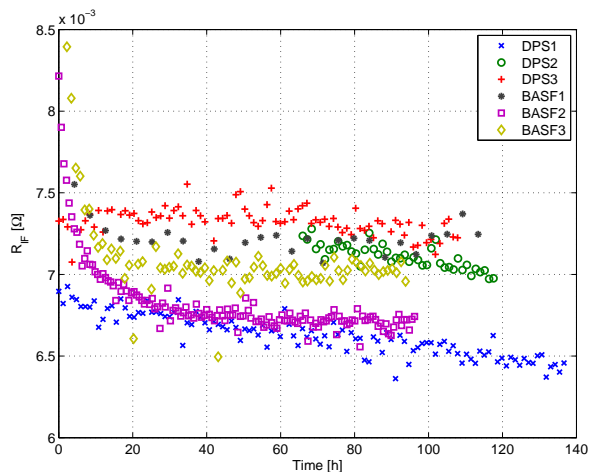

Figure 10: Fitted values of R_{IF} vs. time. Results from model 3.

Warburg resistance. Figure11 shows the fitted values of R_W for all MEAs. As can be seen in the figure, the scatter of the data points is too great to establish any clear development trends. Thus, the Warburg resistance is not a good measure of how well the MEA has been broken in. Assuming that the low frequency capacitive loop is related to convective effects in the flow channels, the lack of significant development of R_W should be expected, since the geometry of the flow field does not change.
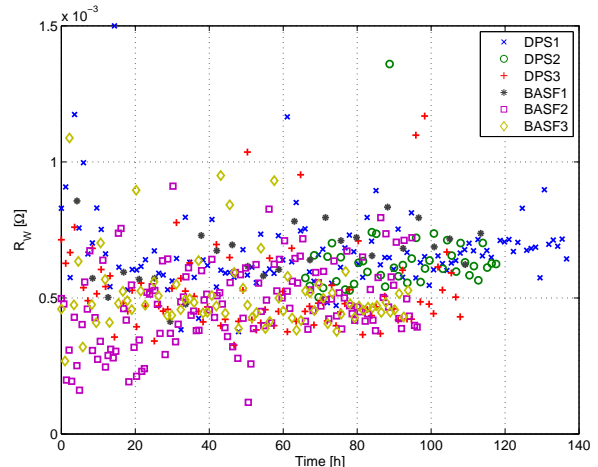

Figure 11: Fitted values of R_W vs. time. Results from model 3.

4. Conclusions

Looking at the fitted resistances, no general, MEA independent break in criterion could be established. This is probably due to the differences in preparation of the MEAs from BASF and DPS. This indicates that the break in criteria must be established individually for each MEA type.

The BASF MEAs seem to have a common tendency towards increasing voltage and decreasing intermediate frequency resistance. The rapid initial part of these changes occur during the first 20 to 30 hours. This does again suggest, that the important part of the break in is over after 30 hours. This means that the break in time of BASF MEAs can most likely be significantly shortened from the official 100 hour recommendation, without causing performance degradation.

The DPS MEAs all exhibit less significant development. The voltage initially decreases, but after some time starts increasing again. Except for a very rapid change during the first hour of break in, the voltage stays within 0.01V throughout the break in period. The intermediate frequency resistance shows a gradual decrease throughout the break in period. This might suggest that no significant activation processes take place in the MEAs after the first hour, and thus they may be ready for use directly from delivery.

Shortening the break in times for all the MEA types could lead to significant savings in the deployment of fuel cell systems. The potential will have to be tested further

by comparing the effects of different break in times on the different MEA types.

[1] S. Galbiati, A. Baricci, A. Casalegno, G. Carcassola, R. Marchesi, On the activation of polybenzimidazole-based membrane electrode assemblies doped with phosphoric acid, International Journal of Hydrogen Energy 37 (19) (2012) 14475–14481, ISSN 03603199, doi:10.1016/j.ijhydene.2012.07.032.

[2] M. Boaventura, A. Mendes, Activation procedures characterization of MEA based on phosphoric acid doped PBI membranes, International Journal of Hydrogen Energy 35 (20) (2010) 11649–11660, ISSN 03603199, doi:10.1016/j.ijhydene.2010.03.137.

[3] K. Kwon, J. O. Park, D. Y. Yoo, J. S. Yi, Phosphoric acid distribution in the membrane electrode assembly of high temperature proton exchange membrane fuel cells, Electrochimica Acta 54 (26) (2009) 6570–6575, ISSN 00134686, doi:10.1016/j.electacta.2009.06.031.

[4] T. Tingelöf, J. K. Ihonen, A rapid break-in procedure for PBI fuel cells, International Journal of Hydrogen Energy 34 (15) (2009) 6452–6456, ISSN 03603199, doi:10.1016/j.ijhydene.2009.05.003.

[5] J. Lobato, P. Cañizares, M. Rodrigo, J. Linares, PBI-based polymer electrolyte membranes fuel cells: Temperature effects on cell performance and catalyst stability, Electrochimica acta 52 (12) (2007) 3910–3920, ISSN 00134686, doi:10.1016/j.electacta.2006.11.014.

[6] J. S. Wainright, J. T. Wang, D. Weng, R. F. Savinell, M. Litt, Acid-Doped Polybenzimidazoles: A New Polymer Electrolyte, Journal of The Electrochemical Society 142 (7) (1995) L121–L123, ISSN 00134651, doi:10.1149/1.2044337.

[7] L. Xiao, H. Zhang, E. Scanlon, L. S. Ramanathan, E.-w. Choe, D. Rogers, T. Apple, B. C. Benicewicz, N. York, High-Temperature Polybenzimidazole Fuel Cell Membranes via a Sol - Gel Process 16 (7) (2005) 5328–5333.

[8] T. J. Schmidt, J. Baurmeister, Properties of high-temperature PEFC Celtec-P 1000 MEAs in start/stop operation mode, Journal of Power Sources 176 (2) (2008) 428–434, ISSN 03787753, doi:10.1016/j.jpowsour.2007.08.055.

[9] S. Simon Araya, S. J. Andreasen, H. V. Nielsen, S. K. Kær, Investigating the effects of methanol-water vapor mixture on a PBI-based high temperature PEM fuel cell, International Journal of Hydrogen Energy 37 (23) (2012) 18231–18242, ISSN 03603199, doi:10.1016/j.ijhydene.2012.09.009.

[10] M. Mamlouk, K. Scott, Mass Transport Characteristics of Cathodes in a Phosphoric Acid Polybenzimidazole Membrane Fuel Cell, Journal of Fuel Cell Science and Technology 8 (6) (2011) 61003, doi:10.1115/1.4004501.

[11] J. Hu, H. Zhang, Y. Zhai, G. Liu, B. Yi, 500 h continuous aging life test on PBI/H3PO4 high-temperature PEMFC, International Journal of Hydrogen Energy 31 (13) (2006) 1855–1862, ISSN 0360-3199, doi:DOI: 10.1016/j.ijhydene.2006.05.001.

[12] X. Yuan, H. Wang, J. C. Sun, J. Zhang, AC impedance technique in PEM fuel cell diagnosis - A review, International Journal of Hydrogen Energy 32 (17) (2007) 4365–4380, ISSN 0360-3199, doi:DOI: 10.1016/j.ijhydene.2007.05.036.

[13] S. J. Andreasen, J. L. k. Jespersen, E. Schaltz, S. K. Kær, Characterisation and Modelling of a High Temperature PEM Fuel Cell Stack using Electrochemical Impedance Spectroscopy, Fuel Cells 9 (4) (2009) 463–473, ISSN 16156846, doi:10.1002/fuce.200800137.

[14] M. Mamlouk, K. Scott, Analysis of high temperature polymer electrolyte membrane fuel cell electrodes using elec-trochemical impedance spectroscopy, Electrochimica Acta 56 (16) (2011) 5493–5512, ISSN 0013-4686, doi:DOI: 10.1016/j.electacta.2011.03.056.

[15] I. A. Schneider, S. A. Freunberger, D. Kramer, A. Wokaun, G. G. Scherer, Oscillations in gas channels Part I. The forgotten player in impedance spectroscopy in PEFCs, Journal of the Electrochemical Society 154 (4) (2007) B383–B388, ISSN 00134651, doi:10.1149/1.2435706.

[16] I. A. Schneider, D. Kramer, A. Wokaun, G. G. Scherer, Oscillations in gas channels II. Unraveling the characteristics of the low frequency loop in air-fed PEFC impedance spectra, Journal of The Electrochemical Society 154 (8) (2007) B770, ISSN 00134651, doi:10.1149/1.2742291.

[17] G. Maranzana, J. Mainka, O. Lottin, J. Dillet, A. Lamibrac, A. Thomas, S. Didierjean, A proton exchange membrane fuel cell impedance model taking into account convection along the air channel: On the bias between the low frequency limit of the impedance and the slope of the polarization curve, Electrochimica Acta 83 (2012) 13–27.

[18] Y. Bultel, L. Géniès, O. Antoine, P. Ozil, R. Durand, Modeling impedance diagrams of active layers in gas diffusion electrodes: diffusion, ohmic drop effects and multistep reactions, Journal of Electroanalytical . . . 527 (2002) 143–155.

[19] S. K. Roy, M. E. Orazem, B. Tribollet, Interpretation of Low-Frequency Inductive Loops in PEM Fuel Cells, Journal of The Electrochemical Society 154 (12) (2007) B1378–B1388, doi:10.1149/1.2789377.

[20] D.-T. Chin, H. Chang, On the conductivity of phosphoric acid electrolyte, Journal of applied electrochemistry 19 (1989) 95–99.

[21] D. MacDonald, J. Boyack, Density, electrical conductivity, and vapor pressure of concentrated phosphoric acid, Journal of Chemical and Engineering Data 14 (3) (1969) 380–384, ISSN 00219568.

[22] S. Galbiati, A. Baricci, A. Casalegno, R. Marchesi, Experimental study of water transport in a polybenzimidazole-based high temperature PEMFC, International Journal of Hydrogen Energy 37 (3) (2012) 2462–2469, ISSN 03603199, doi:10.1016/j.ijhydene.2011.09.159.

[23] C. Wannek, I. Konradi, J. Mergel, W. Lehnert, Redistribution of phosphoric acid in membrane electrode assemblies for high-temperature polymer electrolyte fuel cells, International Journal of Hydrogen Energy 34 (23) (2009) 9479–9485, ISSN 0360-3199, doi:10.1016/j.ijhydene.2009.09.076.

[24] S. Yu, L. Xiao, B. C. Benicewicz, Durability Studies of PBI-based High Temperature PEMFCs, Fuel Cells 8 (3-4) (2008) 165–174, ISSN 16156846, doi:10.1002/fuce.200800024.